

Multi-Approach Study Applied to Restoration Monitoring of a 16th Century Wooden Paste Sculpture

Auxiliadora Gómez-Morón, Pilar Ortiz, Rocio Ortiz, Francesco Colao, Roberta Fantoni, Jacques Castaing, Javier Becerra

▶ **To cite this version:**

Auxiliadora Gómez-Morón, Pilar Ortiz, Rocio Ortiz, Francesco Colao, Roberta Fantoni, et al.. Multi-Approach Study Applied to Restoration Monitoring of a 16th Century Wooden Paste Sculpture. Crystals, 2020, 10 (8), pp.708. 10.3390/cryst10080708 . hal-02941670

HAL Id: hal-02941670
https://hal.sorbonne-universite.fr/hal-02941670

Submitted on 17 Sep 2020

HAL is a multi-disciplinary open access archive for the deposit and dissemination of scientific research documents, whether they are published or not. The documents may come from teaching and research institutions in France or abroad, or from public or private research centers.

L'archive ouverte pluridisciplinaire **HAL**, est destinée au dépôt et à la diffusion de documents scientifiques de niveau recherche, publiés ou non, émanant des établissements d'enseignement et de recherche français ou étrangers, des laboratoires publics ou privés.

crystals

MDPI

Article

Multi-Approach Study Applied to Restoration Monitoring of a 16th Century Wooden Paste Sculpture

Auxiliadora Gómez-Morón [1,2], Pilar Ortiz [2,*], Rocio Ortiz [2], Francesco Colao [3], Roberta Fantoni [3], Jacques Castaing [4] and Javier Becerra [2]

1 Andalusian Historical Heritage Institute, Camino de los Descubrimientos S/N, 41092 Seville, Spain; agommor1@upo.es
2 Department of Physical, Chemical and Natural Systems, Pablo de Olavide University, Utrera Road km 1, 41013 Sevilla, Spain; rortcal@upo.es (R.O.); jbeclun@upo.es (J.B.)
3 ENEA, Department for Fusion and Nuclear Safety Technologies, Division Physical Technologies for Security and Health, Via E.Fermi 45, 00044 Frascati, Roma, Italy; francesco.colao@enea.it (F.C.); roberta.fantoni@enea.it (R.F.)
4 Centre de Recherche et de Restauration des Musées de France and LAMS Université Paris 06 CNRS UPMC UMR 8220, 75000 Paris, France; jacques.castaing@upmc.fr
* Correspondence: mportcal@upo.es; Tel.: +34-954-977-365

Received: 27 July 2020; Accepted: 14 August 2020; Published: 17 August 2020



Abstract: A multi-approach study has been designed to evaluate the mannerist-style masterpiece of the Christ of the Expiration (Museum Brotherhood, Seville, Spain), a polychrome wooden paste sculpture of the 16th Century that was restored in the Andalusian Historical Heritage Institute (IAPH). During its intervention, a combination of two non-destructive prototypes were used to evaluate the different color in its feet regarding its legs and torso and its cause. A portable equipment that combined X-ray diffraction (XRD) and X-ray fluorescence (XRF) was employed to analyze chemical composition and mineralogical characterization of pigments. This equipment allowed obtaining simultaneously XRF and XRD at the same point without sampling. X-ray techniques identified cerussite, hydrocerussite and barite in different layers. The presence of zinc oxide from a recent restoration was also detected. Additionally, laser induced fluorescence (LIF) was employed to assess the presence of different fluorescent compounds on the surface. This technique showed the use of acrylic products in the feet, loincloth and torso of Christ from previous restoration and allowed to detect spectral difference on the feet and a high ration of the acrylic product on feet, both could be the cause of the differential degradation between the feet and torso. This multi-approach study based on portable and non-destructive techniques allowed restoration monitoring and helped restorers to take decisions without sampling.

Keywords: XRD and XRF; Laser Induced fluorescence; wooden paste artworks; portable equipment

1. Introduction

Traditionally, the diagnosis of artworks required sampling to characterize its materials and evaluate its state of conservation. Nevertheless, it is important to develop multi-approach studies that avoid sampling and allow on-site analysis. For that, it is necessary to choose non-destructive and portable techniques whose results are complementary and help restorers to take decisions.

Laser-induced fluorescence (LIF) is a non-destructive technique successfully used to characterize painted surfaces analysis including pigments, organic binders or acrylic resins [1–5] and consolidants [1,6], including the diagnosis on painted surfaces [7,8]. The LIF prototype from ENEA (LidArt), is a lidar fluorosensor (optical radar detecting LIF signals) capable to collect and to analyze the fluorescence induced by ultraviolet laser on remote surfaces [9].

LIF has been combined with Fourier Transform Raman Spectroscopy (FT-RS) to identify pigments and patinas [10–12]. In this paper, LIF has been combined with a prototype from the Centre de Recherche et de Restauration des Musées de France (C2RMF CNRS) that combined X-ray diffraction (XRD) and X-ray fluorescence (XRF) [13,14], capable to measure XRD and XRF at the same point without sampling.

XRD and XRF techniques are broadly employed for the characterization of artworks [15,16], and they are complementary because the first gets crystallographic phases of minerals and the second analyses the chemical composition of materials. Their integration in one instrument performs both analyses simultaneously, using the same radiation source. This equipment have been useful to characterize archaeological materials [17,18], pigments [19,20], ceramics [21] and other materials present such as metal alloys in decorate lacquered furniture or the distribution of silver crystallites in daguerreotypes [22].

In this case, this multi-approach study was carried out in the Christ of Expiration (Figure 1a) a wooden paste sculpture made in 1575. It is a mannerism masterpiece of the sculptor Marcos Cabrera, likely inspired by a drawing of Michelangelo for Vittoria Colonna in 1540, which was well-known in Spain during those years. The image represents the last moments of Christ just before his death on the cross. It was considered an innovation at that time because it was made with lightweight materials (wooden paste) to minimize the weight during its translation in the city on Holy Week and because it was made at full size [23].

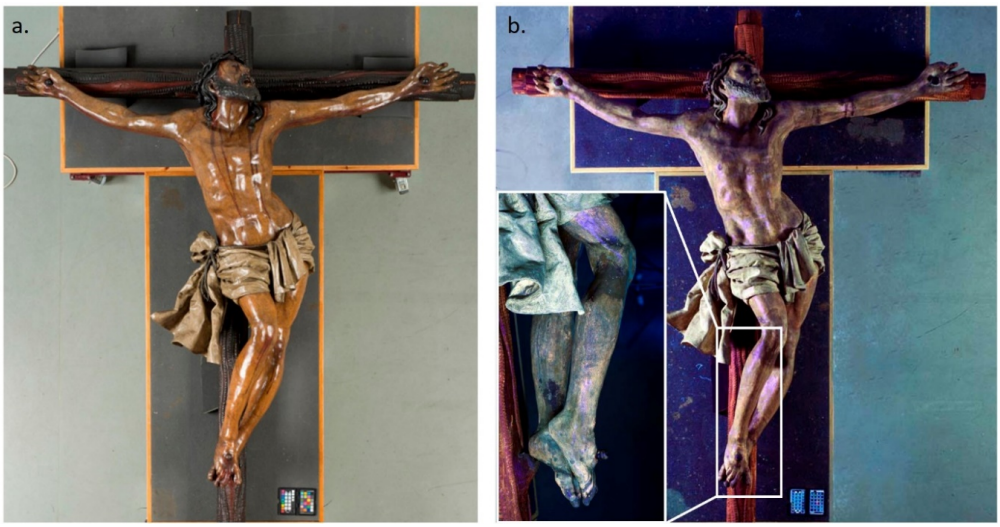


Figure 1. Christ of Expiration (1875 m) under visible light (**a**) and ultraviolet light (**b**). Ultraviolet light was used to detect previous interventions due to the different fluorescence of the materials. Inset, a detail of the leg of the sculpture where was possible to see the last intervention (darkening areas).

This wooden paste has clearly an intangible value as it was designed for processional purpose. Even nowadays, after four centuries, the Museum Brotherhood from Seville (Spain) maintains the devotion and its processional use on Monday during Holy Week.

The image suffered several interventions between 1893 and 1895, which fixed the current profile of the sculpture. Afterwards, several restorations have been documented: (a) Manuel Gutierrez Reyes Cano made a new loincloth in 1895, (b) Francisco Peláez Del Espino carried out several interventions in 1978, 1985 and 1988. From April 1990 to March 1991 the Institute of Conservation and Restoration of Cultural Heritage (IPCE) restored the image. Luis Alvarez Duarte repaired the damage on feet and legs due to the dents suffered after a blow in 2008 [23].

The image showed a differential alteration of the painted layers from different interventions, that produce a yellowish tone, mainly located on legs and feet. These interventions are not clearly located by ultraviolet light (Figure 1b). It was necessary to characterize the pigments and varnishes on the whole surface without taking samples. Therefore, chemical and mineralogical information should be

obtained by means of non-destructive analytical techniques, improving diagnosis of the artwork before and during its intervention [24].

The use of both techniques, LF and XRF-XRD, was a challenge due to the shape and the nature (wooden paste) of the sculpture [20] and this multi-approach was compared with the classical methodology based on sampling and traditional techniques in order to assess the improvement of diagnosis of an artwork before and during its interventions. These traditional techniques were optical microscopy, scanning electron microscopy-energy dispersive X-ray spectroscopy (SEM-EDX) and infrared spectroscopy (FTIR) applied on samples taken from zones with cracks and fissures.

2. Materials and Methods

2.1. Study by Traditional Techniques (OM, FTIR and SEM-EDX)

In order to compare the results of LIF and XRF-XRD techniques with traditional techniques used in the diagnosis of Cultural Heritage, a few samples were taken in cracks or lagoon borders, according to the European standard EN 16085 [25]. Samples were embedded in methyl-methacrylate resin to observe the cross-section and were studied with a stereoscopic microscope, an optical microscope (OM) with reflected light Leika DM5500 (Leika Microsystem, Seville, Spain) using normal light and ultraviolet light (UV (360 nm), Leika A 106 Z, Leika Microsystem, Seville, Spain) and a scanning electron microscope (SEM) JSM 5600 LV (JEOL, Seville, Spain) with elemental microanalysis by energy dispersive X-ray (EDX) Inca X-Sight (Oxford Instruments, Seville, Spain) to determine the elemental composition of the pigments and inorganic fillers.

Infrared spectroscopy with Fourier Transform Perkin Elmer Spectrum 100 was carried out to study coatings or varnishes. Analyses were performed between 4400 cm^{-1} and 370 cm^{-1}, with KBr pellets or by surface analysis using UATR (Universal Attenuated Total Reflectance) technique.

Eight samples were taken from the sculpture to evaluate the color palette of polychromies and to identify the constituent materials (EXPQx, Figure 2). Unfortunately, as could be seen later, there was no sample on the feet due to the lack of any crack or lagoon in this area.

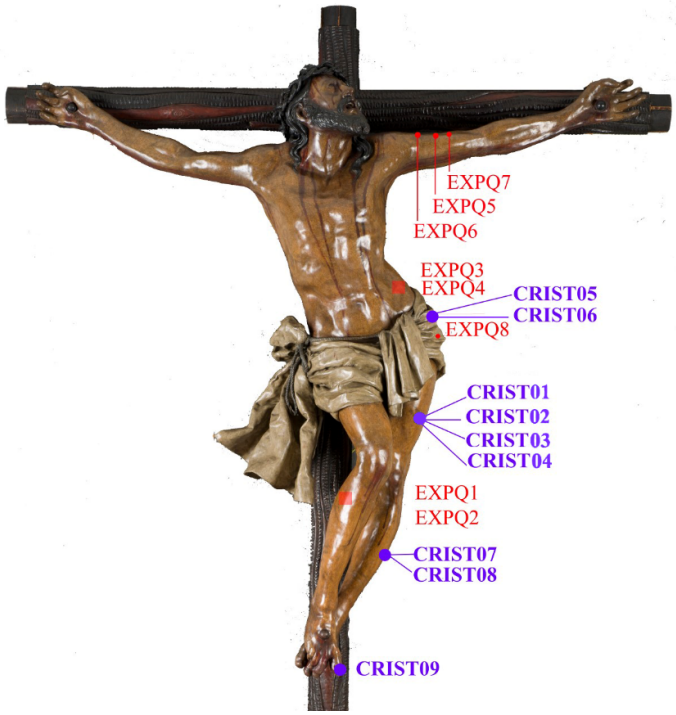


Figure 2. General view of Christ of Expiration and location of the different analyses. XRF-XRD zone of the study (code CRISTxx in purple) and traditional sampling (code EXPQx in red) in the surface of the Christ of Expiration.

2.2. Study by Laser Induced Fluorescence

A Laser Induced Fluorescence prototype from ENEA [9], that collects hyperspectral fluorescence images induced by a laser beam, was used in this study. The system scans a zone to identify the fluorescence signature of surface without sample taking [6,26–30]. This prototype was used to evaluate the varnish applied during the last restoration that was getting darker on legs and feet [31,32], as this could not be identified by classic techniques as UV photography (Figure 1b) [24].

The system was set up to detect the spectral signature of sculpture surface in its own church before the restoration. To this end, the laser was set up to emit in the UV at 266 nm, while detector acquired the full spectrum from 200 nm to 850 nm with a spectral resolution of 2.5 nm. The Laser average power was 0.9 mJ/pulse at 20Hz, the energy density at target plane 0.2 mW/cm^2, the Spectrograph was a Horiba CP-140 and the detector an ICCD Andor DH734-18F.

Successive scans have been performed on the images with the aim to measure both the reflectance and the laser induced fluorescence. All reflectance images were acquired in low resolution mode, since they were only used to better identify the scanned portion.

The detection of the emitted fluorescence identified the presence of substances excited by UV radiation: biodeterioration, pollutant, waxes, pigments and surface treatments [6,31,32].

2.3. Study by XRF-XRD

A portable XRD and XRF apparatus has been used to characterize chemical and mineralogical composition of the pigments. This equipment allows simultaneously crystallographic structure identification and elemental chemical analysis in the same place without sample taking. The portable XRF-XRD system was developed by the C2RMF with the support of the European projects EU-ARTECH (EU FP 6 RII3-CT-2004-506171, [33]) and has been used within MOLAB (EU CHARISMA program FP7-228330 [34]).

X-rays are produced with a Cu anode source. XRF elemental analysis is performed with a SDD detector with a resolution of 150 eV FWHM at 5.9 KeV. X-ray diffractograms are collected in reflection with the beam at 10° from the surface. The beam spot on the surface is about 3 mm in diameter [13,14]. Figure 3 shows the experimental system.

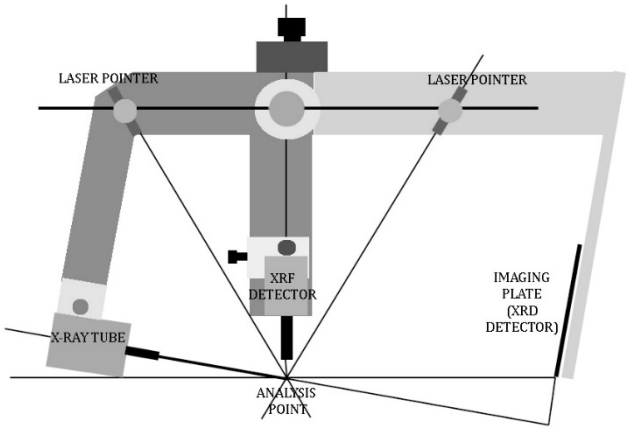


Figure 3. Experimental system of the prototype developed by the C2RMF to analyze simultaneously elemental chemical analysis (XRF) and crystallographic structure identification (XRD).

With this prototype and conditions, the thickness of analyzed materials is directly related to the penetration of X-rays. Taking into account the angle between the incident X-ray beam and the object surface (≈10°), we estimate that XRD (8.05 keV) is performed on a 20 µm thick layer of containing mostly light elements (Al, Si, K, …) and 5 µm for heavy elements (Pb, Hg, Sn, …) [14].

For XRF, depth of analysis depends not only on the elements, but also on the X-ray energies that are used. As an example, a 100 µm thick organic layer is transparent to Pb-L X-rays (10–15 keV

energy) and opaque to Pb-M X-ray (about 2 keV). The additional challenge in this case is to check if it is possible obtain information of the various layers due to interventions without taking samples during the restoration processes, as stratigraphies showed a preparation layer of 200 µm, a lead white layer of 200 µm and then the color layer of 200–220 µm [35].

In the painting surface were analyzed four areas with different varnishes and the original layer by XRF-XRD. A total of eight measures were taken in the sculpture (CRISTxx, Figure 2). XRF-XRD selected points depended on the palette, the restorations, the curvature of the sculpture and the dimensions of the equipment, which are best adapted to analysis in flat zones.

A stratigraphic analysis was made in three of the studied areas corresponding to zones where varnishes and repaintings were progressively cleaned away, one on the leg, one on the thigh and one on the loincloth (Figure 2). In each case, we have compared the level at the bottom of the cleaned zone with the current surface of cleaning tests. It was possible because during the cleaning tests, the restorers removed successive polychrome layers in small areas. This allows analyzing the different layers by these non-destructive techniques (XRF-XRD). The first cleaning test was performed in the left thigh. The varnish layer (CRIST01), the outer unvarnished polychrome layer (CRIST02), the following polychrome layer (CRIST03) and the layer considered as original polychrome (CRIST04) were analyzed. The second cleaning test has been made in the loincloth where we have analyzed two points (CRIST05 and CRIST06). The third cleaning test was performed in the left calf where dirty surface has been removed and measurements have been performed in the darkened area and the cleaned one (CRIST07 and CRIST08) (Figure 2). The last point has been analyzed in the big toe of his right foot (CRIST09), with all the layers.

3. Results and Discussion

3.1. Study by Traditional Techniques (OM, FTIR and SEM-EDX)

UV and visible light microscope observation showed a preparation layer consisting of animal glue, detected by FTIR, while SEM-EDX showed the signal of sulfur and calcium, likely due to plaster [36] (Figure 4 and Table 1).

The color palette identified by traditional techniques (FTIR and SEM-EDX) appears in Table 1. For example, red colors were due to red lake and iron, although the presence of silicon and aluminum were likely due to red earth. Red lake is a general term that includes lakes with different compositions and origins, such as cochineal lake, madder lake, etc. In this study, it was possible to identify a red pigment as red lake because of the lakes have a characteristic fluorescence under UV light (OM equipped with UV light). Inorganic red pigments, such as hematite, vermillion or minium, do not have fluorescence. Additionally, this identification was confirmed by FTIR, and the calcium detected by SEM-EDX probably correspond to calcite, an usual substrate to the dyestuff [37].

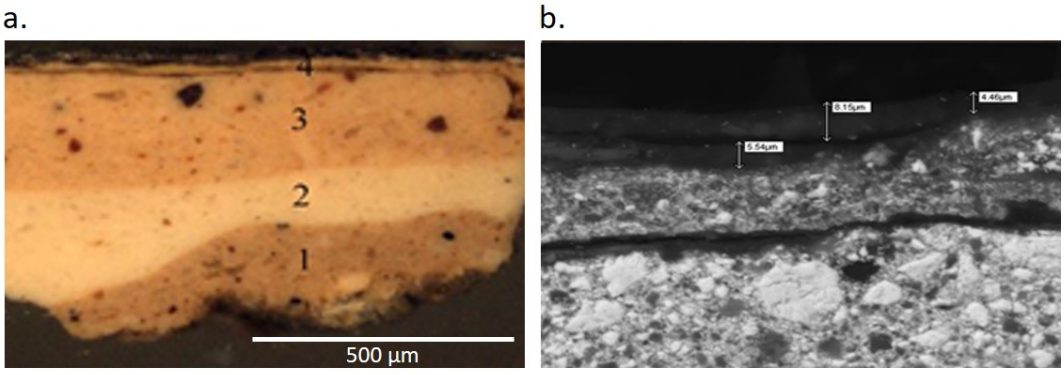


Figure 4. Stratigraphy of Sample EXPQ1 from the leg. (**a**). Optical microphotography shows the presence of four layers. (**b**). SEM-EDX detail of the upper layers that contained two layers of acrylic resin with iron oxide pigments applied in the last restoration to homogenize the color [38].

Table 1. Results of traditional techniques (OM, SEM-EDX, FTIR).

Sample	Description	OM Stratigraphy	Thickness μm	Elements Detected by SEM-EDX *	Suggested Materials
EXPQ5	Carnation left arm	Brown primer	50	Ca, S	Gypsum, animal glue
		Pink layer	200	Pb, Al, Ca, K, Si	Lead white, red lake, calcite grains, quartz grains
		White layer	200–220	Pb, Si, Ca,	Lead White, calcite grains, quartz grains
		Pink layer	30	Pb, Si, Fe, Ca, Al, K, Mn	Lead White, earth red pigment, hematite, red lake, calcite grains, quartz grains, raw umber
		Pink layer	25	Pb, Si, Fe, Ca, Al, K	Lead White, earth red pigment, hematite, red lake, calcite grains, quartz grains
EXPQ6	Transparent-yellowish final layer. Varnish scraped with scalpel			Ca, Fe, Mn, Si, S, Ba, Zn, P, Al, Na, K	Hematite, earth red pigment, barite and zinc white, raw umber, bone black (known commercially as Vandyke brown)
EXPQ7	Carnation left arm	Brown primer	90–200	Ca, S	Gypsum, animal glue
		white layer	45–125	Pb, Ca, K, Si	Lead white, calcite grains, quartz grains
		Pink layer	200–225	Pb, Fe, al, Si, K, Ca,	Lead White, hematite, earth red pigment, red lake, calcite grains, quartz grains
		Pink layer	30	Pb, Si, Fe, Ca, Al, K, Mn	Lead White, earth red pigment, hematite, red lake, calcite grains, quartz grains

* Elements reported in bold characters are the most abundant in the layer.

Considering the polychromatic sequence, the original carnation consists on white lead and red lake and iron oxide pigments with small amounts of calcite and quartz grains. The thickness of this layer varies between 90 and 200 μm. Every sample showed a second layer composed of lead white, grains of quartz and calcite with a thickness ranging between 45 and 200 μm. On this layer a double layer made by white lead, red lake, red earth and hematite with some grains of calcite and quartz was located. This third layer has a thickness between 200 and 225 μm. The outermost painting layer has a composition very similar to the above composition, consisting on white lead, red lake, red earth and hematite with some grains of calcite and quartz, but applied roughly with a small thickness, between 25 and 30 μm. The presence of white pigments based on barite and zinc white was interpreted as a repainting layer (EXPQ06).

Varnishes were identified by FTIR (Table 2). Between the second painting layer and the last one two layers of acrylic resin with iron oxide pigments were identified. These layers may be applied to homogenize the color in the last restoration [39].

Table 2. Results of IR.

Sample	Description	Characteristic Infrared Bands cm^{-1}	Suggested Materials
EXPQ1	Transparent-yellowish final layer. Varnish scraped with scalpel.	2918, 2850, 1723, 1448, 1383, 1244, 1140, 1115, 1023, 679	Acrylic resin
EXPQ2	Second layer of varnish, Transparent-yellowish (scraped with scalpel).	2918, 2850, 1723, 1448, 1383, 1244, 1140, 1115, 1023, 679	Acrylic resin
EXPQ3	Transparent-yellowish final layer. Varnish scraped with scalpel.	2918, 2850, 1723, 1448, 1383, 1244, 1140, 1115, 1023, 679	Acrylic resin
EXPQ4	Second layer of varnish, Transparent-yellowish (scraped with scalpel).	2918, 2850, 1723, 1448, 1383, 1244, 1140, 1115, 1023, 679	Acrylic resin

3.2. Study by Laser Induced Fluorescence

Figure 5 shows the reflectance images and scanning LIF image taken from the right angle on the altar of Christ of Expiration in his Chapel Museum. This technique allowed working on-site avoiding the risk of transport and manipulation of artworks.

The reflectance image shows the cloth covering the altar and generates a strong fluorescence signal which has forced to reduce areas of statistical analysis to avoid the influence of this background. Therefore, LIF image has framed the area of study (Figure 5c). This zone has been subjected to spectral study and similarities by PCA [40–42].

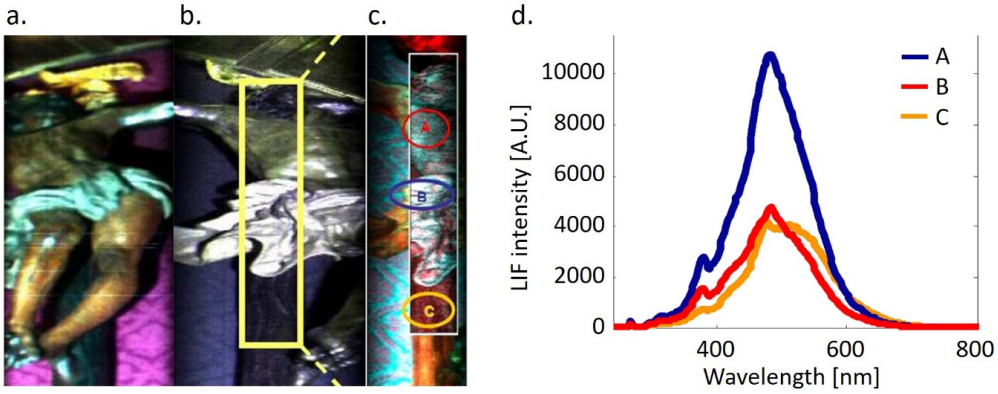


Figure 5. (**a**). Reflectance image. (**b**) LIF image with the zone for PCA study. (**c**). Zones for Spectral scanning body (A), loincloth (B), cross (C). (**d**). LIF spectra taken from different areas of the Christ body (A), loincloth (B), cross (C).

Statistical studies of spectral similarity reveal a product in the torso and the loincloth that is not on the cross (Figure 5d). This product is characterized by a signal 370 nm, that could be due to a weak presence of acrylic resins [30,35]. All the zones of study present a large emission at 480 nm that need data base for further studies [1,4,10]. The darkening agent observed by naked eye, dominating on Christ's body and loincloth but absent on the cross, might be related to a degraded product of the acrylic resin (small signature at 370 nm and large visible emission at 480 nm). The presence of acrylic resin agrees with the results obtained by the traditional techniques (FTIR), as could be seen later. For that, LIF results allowed taking decisions to the restorers based on a whole analysis instead on samples.

In order to understand the differences between the feet and body, Figure 6 includes a RBG image from reflectance measurement with the purpose of matching the pixel spectral features with the exact location in the scanned image (a), a false color LIF image of the scanned body from a perspective view showing the head, body, loincloth and legs (b), full detailed LIF image (as before) including the background (c), and finally, a cumulative content of peak intensity at 370 nm obtained from PC2 along

a line from the head trough the torso, the loincloth and the legs (d). The false color LIF image has been obtained associating the RGB channels to the components 1, 2 and 3 of the PCA.

Yellowish areas observed on feet are mostly correlated with prominence of the peak at 370 nm. The LIF results show difference between the concentrations of this acrylic product, as the ratio to the visible component is much different between the torso and the feet. Indeed, the ratio was roughly 1:3 on the torso, while on the feet it was much larger 1:1 (Figure 6b). This might suggest that the feet were more heavily restored in a former treatment and may be the cause of the darkening in this zone. In order to improve the rightmost plot of Figure 6, it would be necessary to have a better deconvolution of the peak at 370 nm.

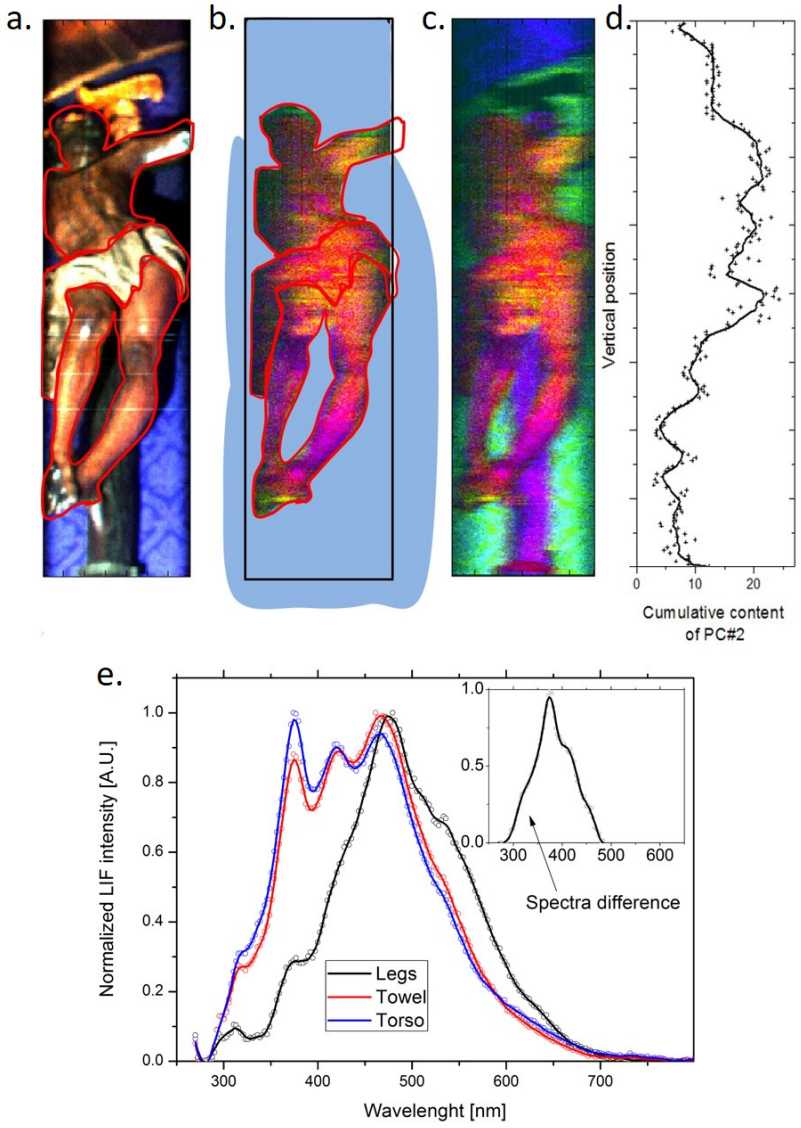


Figure 6. (**a**). RBG image from reflectance measurement. (**b**). False color LIF image. (**c**). False color LIF image including the background. (**d**). Cumulative content of peak intensity at 370 nm obtained from PC2. (**e**). Spectral difference of the torso/leg/towel at 370 nm.

The analysis shows a rather large difference (more than double) in the integrated intensity of the principal component (PC2) associated with the F370 peak. The spectral difference of the torso/leg shows a prominent peak at 370 nm, which is consistent with use of varnished layer on the surface. Moreover, a strong dissimilarity on legs and on torso was revealed by Figure 6e, which implies different restoration products on the feet or degradation processes, though the current databases do not allow

further identification. It would be presumably the result of a chemical interaction with constituents on the inner layers and/or other superficial chemicals; in any case, it shows almost the same effects as an accelerated ageing.

The conclusion is that the superficial layer has undergo to a deterioration process caused by the accelerated ageing of acrylic products. LIF analysis gives a strong indication that the layer composition is different on the torso and in the legs, and this may explain the change in visible color that could not be studied by traditional techniques. In this sense, the color changes in the sculpture were caused by the ageing of the protective products (superficial layer) and no by the deterioration of the polychrome. This information was very valuable for restorers to design the cleaning process during the restoration.

3.3. Study by XRF-XRD and Comparison with Traditional Techniques

On-site XRF spectra detect the presence of Ca, Fe, Pb, Zn, Ba, Mn and Sr. Most of them have been confirmed by SEM-EDX, while Sr was not detected by the SEM-EDX.

On site XRD showed the following minerals: hydrocerussite ($2PbCO_3 \cdot Pb(OH)_2$), cerussite ($PbCO_3$), hematite (Fe_2O_3), calcite ($CaCO_3$), zinc white or zinc oxide (ZnO), barite ($BaSO_4$) and manganese oxide (MnO). The chemical elements identified by SEM-EDX, and their interpretation, confirmed the presence of lead white, calcite, zinc white and hematite.

Red earth (aluminosilicates with iron) could not be detected by our XRF-XRD prototype, as the device is not able to detect the level signals of clays and X-ray of low energy (<2 Kev), unless this element were in high concentration [18].

XRF of two cleaned areas in Christ's leg shows that the calcium line is the strongest in the lowest layer (likely preparation layer) and lead white appears in all the layers according to stratigraphies. The results show that the L lines of lead (Pb-L) are identical at all points analyzed, while the M lines of lead become more intense as we reach the cleaned zone (Figure 7). The Pb-M line has been absorbed by the upper layer and its intensity is reduced according to Lognoli et al. [26], this indicates that there is no (or less) Pb in the first layer (varnish and/or last restoration) while it is present on the deep layers (original and previous restoration) [43].

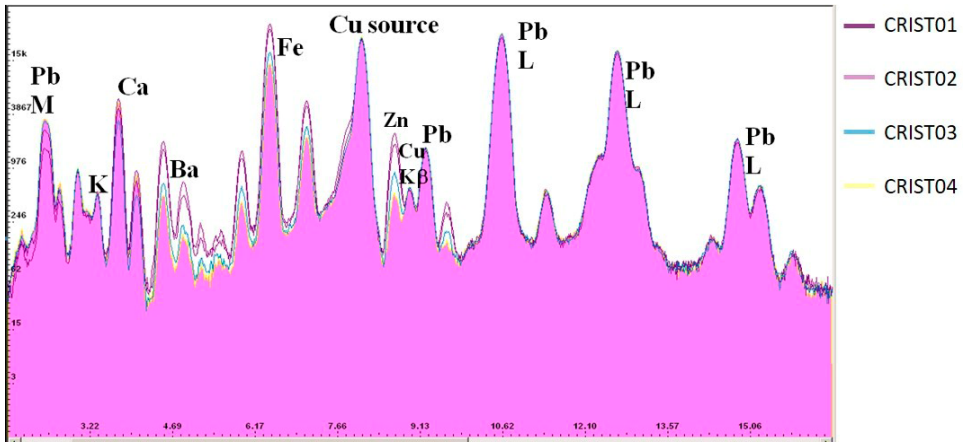


Figure 7. XRF spectrum of samples Crist01-Crist04, from the upper layer to the cleanest zone (Crist04). Pb has maximum concentration in the cleanest layer; conversely, Ba, Mn, Fe and Zn have minimum concentration in the cleaned layer.

Similar results appeared on the toe surface. The XRF spectrum shows a Pb-L line very weak in comparison with Pb-M line, which shows that white lead is not on the most external layer. Therefore, an additional layer was added in the restoration of Luis Alvarez Duarte in 2008.

The toes XRD results reveal a high content of barite with average amounts of calcite and zinc white. This has been confirmed by EDX-SEM and OM (Figure 4). White lead minerals are not detected in the toe restoration by XRD because it is in small quantity and/or below the barite layer.

Ba, Mn, Fe and Zn XRF lines present maximum intensity in uncleaned zones indicating that these elements are part of the varnish used in the lasts restoration to homogenize the color according to traditional techniques that employed hematite and fillers mixed with varnishes to provide color.

The analyses of X-ray fluorescence in loincloth points also indicate that the coating contains Ca, Fe and Zn, with a high content of Ba. These results might imply that also the loincloth was retouched in a previous restoration or it may be included by Manuel Gutierrez Reyes Cano in 1895, as white zinc began to substitute lead white for its toxicity. Nevertheless, lead white has been detected by XRD.

Figure 8a shows the XRD spectra acquired in the cleaned zone without varnish (CRIST07, black line) and in the area with varnish (CRIST08; red line). Both diagrams are almost identical, with the presence of hidrocerussite/cerussite (white lead) and barite in both. The presence of white lead in the uncleaned zone is due to the acquisition conditions where diffractogram acquires not only the varnish signal but also comes from the deeper layers, which contain this compound according to the results obtained in the XRF spectrum.

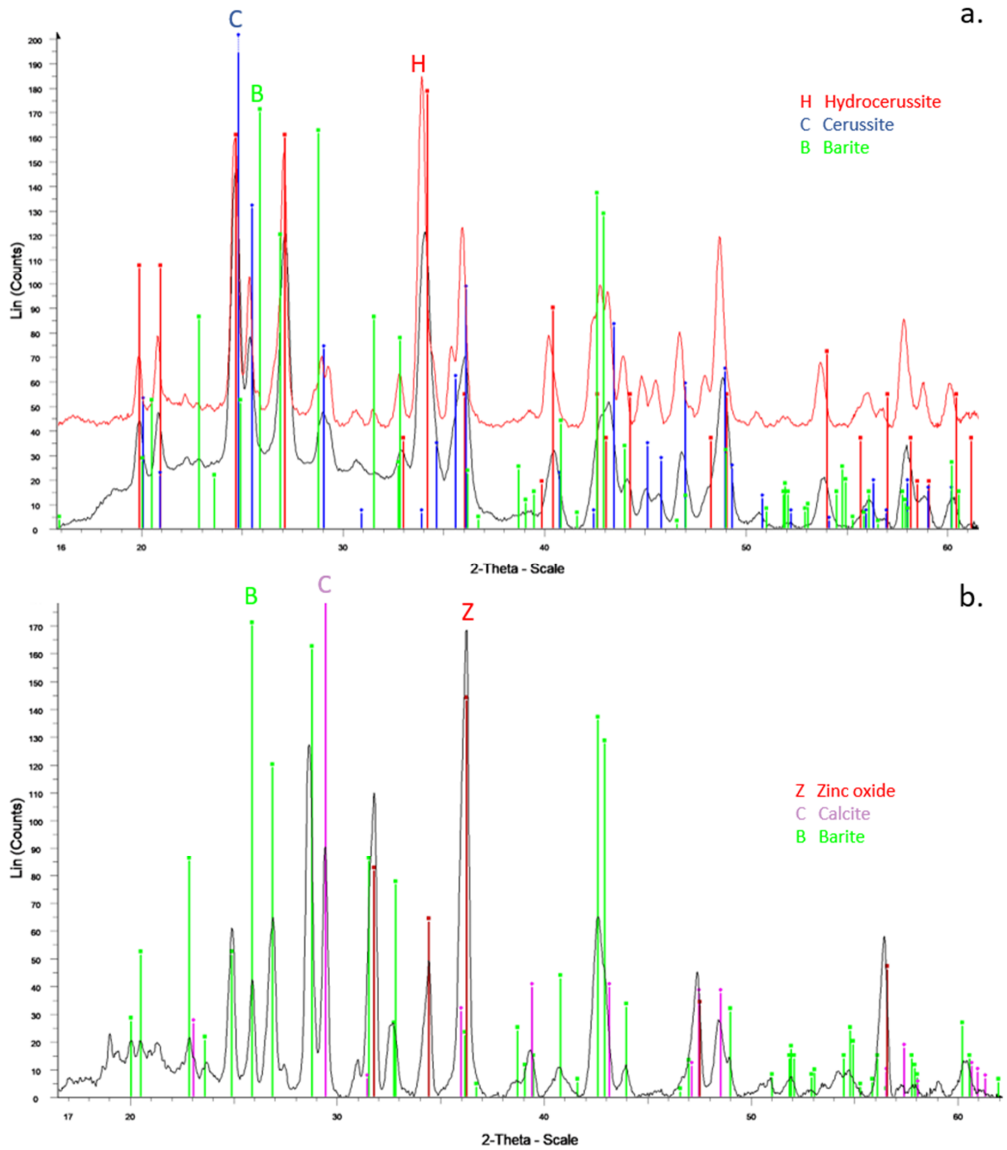


Figure 8. (**a**). XRD diagram shows the presence of hidrocerussite (red vertical lines), cerussite (blue vertical lines) and barite (green vertical lines) in CRIST07 (black spectra) and CRIST08 (red spectra) zones. (**b**). XRD diagram shows the presence of calcite (purple vertical lines), barite (green vertical lines) and zinc oxide (red vertical lines) in CRIST09 zone.

XRD diagrams are dominated by cerussite and hydrocerussite which implies that acid products are not admissible during the restoration, as they are composed by carbonates. These results, crucial for restorers, usually are estimated by SEM-EDX as lead is detected by traditional techniques as SEM-EDX, thought the mineralogical composition is not known. Conversely, FRX-XRD prototype allow both chemical and mineralogical information.

Finally, XRF of a repainting area on the toe contains mainly Ca, Ba and Zn that correspond with calcite, barite and zinc oxide (Figure 8b). Barite appears in small quantities and it is most likely located in the varnish layer. The lack of iron might be due to the use of organic pigments, such as the red lake detected by IR on other zones.

The natural oxidation of the varnish and a possible alteration of the red lake could be the cause of the yellowish tone, mostly on legs and feet that began to get a darker tone than the rest of the image. This alteration may be worsened by added pigments to give color to the varnish during the last restoration.

Table 3 summarizes the results obtained by traditional techniques and XRF-XRD prototype.

Table 3. Main color composition detected by XRF-XRD prototype and comparison with traditional techniques (OM, FTIR and SEM-EDX).

Color	XRF-XRD	Traditional Techniques (FTIR, OM, SEM-EDX)
White	Barite, hidrocerussite and cerussite, calcite, zinc oxide.	white lead calcite, zinc white
Red	Fe in XRF (hematite)	Red lake, red earth, hematite
Brown	Mn in XRF manganese oxide (MnO)	Manganese oxide

NOTE: White lead or hydrocerussite ($2PbCO_3{\cdot}Pb(OH)_2$), calcite ($CaCO_3$), zinc white or zinc oxide (ZnO), barite ($BaSO_4$), cerrussite ($PbCO_3$), red lake (organic pigment), red earth (aluminosilicates with iron), manganese oxide (MnO).

4. Conclusions

The combination between LIF and portable XRF-XRD allows to assess the presence of some original, restoration and repainting products whose information is very useful for restoration and could reduce the number of samples.

The LIF study made over the sculpture surface shows specific difference on spectral signatures. In this case, a product with a similar nature was applied on the loincloth and torso of Christ and, in more quantity, on feet. Furthermore, LIF results suggested a differential alteration of the acrylic resins what allowed restorers to conclude that the color difference was not due to the alteration of the polychrome.

XRD and XRF portable prototype performed minerals and chemical analysis without sampling and in the same point. In this case, cerussite, hydrocerussite and barite were identified at different layers, in comparison with traditional techniques that only allowed assuming the presence of lead white and barite. Furthermore, ZnO was also detected and associated to the last restoration. The interpretation of the stratigraphic helped to restorers to decide what layers were associated to previous interventions and which should be removed.

The combination of these two prototypes (LIF and XRF-XRD) is advisable for good diagnosis practice before and during the cleaning test, to perform the chemical and mineralogical characterization of the surface without risk of damage the artwork and without sampling. This information was used by restorers to design the restoration of the sculpture, especially the cleaning process.

Author Contributions: Conceptualization, A.G.-M., P.O., R.O., J.B.; methodology, A.G.-M., P.O., R.O., F.C., R.F., J.C., J.B.; software, F.C., R.F., J.C.; validation, A.G.-M., P.O., R.O., F.C., R.F., J.C., J.B.; investigation A.G.-M., P.O., R.O., F.C., R.F., J.C., J.B.; resources, P.O.; data curation, A.G.-M., P.O., R.O., F.C., R.F., J.C., J.B.; writing A.G.-M., P.O., R.O., F.C., R.F., J.C., J.B.; supervision, P.O.; project administration, P.O.; funding acquisition, P.O. All authors have read and agreed to the published version of the manuscript.

Funding: This research was funded by JUNTA DE ANDALUCIA, grant number HUM-6775 (RIVUPH), and MINISTERIO DE ECONOMíA Y COMPETITIVIDAD AND FONDO EUROPEO DE DESARROLLO REGIONAL, grant number BIA2015-64878-R (Art-Risk).

Acknowledgments: This study has been partially supported by the agreements IAPH&UPO and ENEA&UPO. M.A. Gómez-Morón is grateful by her researcher stay in ENEA, funded by Cei Patrimonio, and R. Ortiz by her researched stay in IAPH. The researchers are grateful to the graphic archive of IAPH for the photographs of the Christ of the Expiration (Figures 1 and 2).

Conflicts of Interest: The authors declare no conflict of interest. The funders had no role in the design of the study; in the collection, analyses, or interpretation of data; in the writing of the manuscript, or in the decision to publish the results.

References

1. Borgia, I.; Fantoni, R.; Flamini, C.; Di Palma, T.M.; Guidoni, A.G.; Mele, A. Luminescence from pigments and resins for oil paintings induced by laser excitation. *Appl. Surf. Sci.* **1998**, *127–129*, 95–100. [CrossRef]
2. Nevin, A.; Cather, S.; Anglos, D.; Fotakis, C. Analysis of protein-based binding media found in paintings using laser induced fluorescence spectroscopy. *Anal. Chim. Acta* **2006**, *573–574*, 341–346. [CrossRef] [PubMed]
3. Nevin, A.; Anglos, D. Assisted Interpretation of Laser-Induced Fluorescence Spectra of Egg-Based Binding Media Using Total Emission Fluorescence Spectroscopy. *Laser Chem.* **2006**, *2006*, 1–5. [CrossRef]
4. Anglos, D.; Solomidou, M.; Zergioti, I.; Zafiropulos, V.; Papazoglou, T.G.; Fotakis, C. Laser-Induced Fluorescence in Artwork Diagnostics: An Application in Pigment Analysis. *Appl. Spectrosc.* **1996**, *50*, 1331–1334. [CrossRef]
5. Marinelli, M.; Pasqualucci, A.; Romani, M.; Verona-Rinati, G. Time resolved laser induced fluorescence for characterization of binders in contemporary artworks. *J. Cult. Herit.* **2017**, *23*, 98–105. [CrossRef]
6. Fiorani, L.; Caneve, L.; Colao, F.; Fantoni, R.; Ortiz, P.; Gómez, M.A.; Vázquez, M.A.; Gomez, M.A.; Vazquez, M.A.; Gómez, M.A.; et al. Real-Time Diagnosis of Historical Artworks by Laser-Induced Fluorescence. *Adv. Mater. Res.* **2010**, *133–134*, 253–258. [CrossRef]
7. Comelli, D.; Nevin, A.; Valentini, G.; Osticioli, I.; Castellucci, E.M.; Toniolo, L.; Gulotta, D.; Cubeddu, R. Insights into Masolino's wall paintings in Castiglione Olona: Advanced reflectance and fluorescence imaging analysis. *J. Cult. Herit.* **2011**, *12*, 11–18. [CrossRef]
8. Comelli, D.; D'Andrea, C.; Valentini, G.; Cubeddu, R.; Colombo, C.; Toniolo, L. Fluorescence lifetime imaging and spectroscopy as tools for nondestructive analysis of works of art. *Appl. Opt.* **2004**, *43*, 2175–2183. [CrossRef]
9. Colao, F.; Fantoni, R.; Fiorani, L.; Palucci, A. Portable fluorescence device for space scanning of surfaces, especially for cultural heritage applications "Dispositivo portatile a fluorescenza per la scansione spaziale di superfici, in particolare nell'ambito dei beni culturali". RM2007A000278, 2007.
10. Domingo, C.; Silva, D.; García-Ramos, J.V.; Castillejo, M.; Martín, M.; Oujja, M.; Torres, R.; Sánchez-Cortés, S. Spectroscopic Analysis of Pigments and Binding Media of Polychromes by the Combination of Optical Laser-Based and Vibrational Techniques. *Appl. Spectrosc.* **2001**, *55*, 992–998.
11. Oujja, M.; Vázquez-Calvo, C.; Sanz, M.; de Buergo, M.Á.; Fort, R.; Castillejo, M. Laser-induced fluorescence and FT-Raman spectroscopy for characterizing patinas on stone substrates. *Anal. Bioanal. Chem.* **2012**, *402*, 1433–1441. [CrossRef]
12. Syvilay, D.; Bai, X.S.; Wilkie-Chancellier, N.; Texier, A.; Martinez, L.; Serfaty, S.; Detalle, V. Laser-induced emission, fluorescence and Raman hybrid setup: A versatile instrument to analyze materials from cultural heritage. *Spectrochim. Acta Part B At. Spectrosc.* **2018**, *140*, 44–53. [CrossRef]
13. Eveno, M.; Moignard, B.; Castaing, J. Portable apparatus for in situ x-ray diffraction and fluorescence analyses of artworks. *Microsc. Microanal.* **2011**, *17*, 667–673. [CrossRef] [PubMed]
14. Gianoncelli, A.; Castaing, J.; Ortega, L.; Dooryhée, E.; Salomon, J.; Walter, P.; Hodeau, J.-L.; Bordet, P. A portable instrument for in situ determination of the chemical and phase compositions of cultural heritage objects. *X-ray Spectrom.* **2008**, *37*, 418–423. [CrossRef]
15. Ferrett, M. X-ray Fluorescence Applications for the Study and Conservation of Cultural Heritage. In *Radiation in Art and Archeometry*; Creagh, D.C., Bradley, D.A., Eds.; Elsevier: Amsterdam, The Netherlands, 2000; pp. 285–296. [CrossRef]

16. Artioli, G. Science for the cultural heritage: The contribution of X-ray diffraction. *Rend. Lincei* **2013**, *24*, 55–62. [CrossRef]
17. Lutterotti, L.; Dell'Amore, F.; Angelucci, D.E.; Carrer, F.; Gialanella, S. Combined X-ray diffraction and fluorescence analysis in the cultural heritage field. *Microchem. J.* **2016**, *126*, 423–430. [CrossRef]
18. Mendoza Cuevas, A.; Bernardini, F.; Gianoncelli, A.; Tuniz, C. Energy dispersive X-ray diffraction and fluorescence portable system for cultural heritage applications. *X-ray Spectrom.* **2015**, *44*, 105–115. [CrossRef]
19. Uda, M. In situ characterization of ancient plaster and pigments on tomb walls in Egypt using energy dispersive X-ray diffraction and fluorescence. *Nucl. Instrum. Methods Phys. Res. Sect. B Beam Interact. Mater. Atoms* **2004**, *226*, 75–82. [CrossRef]
20. Van De Voorde, L.; Van Pevenage, J.; De Langhe, K.; De Wolf, R.; Vekemans, B.; Vincze, L.; Vandenabeele, P.; Martens, M.P.J. Non-destructive in situ study of "mad Meg" by Pieter Bruegel the Elder using mobile X-ray fluorescence, X-ray diffraction and Raman spectrometers. *Spectrochim. Acta Part B At. Spectrosc.* **2014**, *97*, 1–6. [CrossRef]
21. Gómez-Morón, M.A.; Ortiz, P.; Martín-Ramírez, J.M.; Ortiz, R.; Castaing, J. A new insight into the vaults of the kings in the Alhambra (Granada, Spain) by combination of portable XRD and XRF. *Microchem. J.* **2016**, *125*, 260–265. [CrossRef]
22. Chiari, G.; Sarrazin, P.; Heginbotham, A. Non-conventional applications of a noninvasive portable X-ray diffraction/fluorescence instrument. *Appl. Phys. A Mater. Sci. Process.* **2016**, *122*, 990. [CrossRef]
23. Pérez del Campo, L.; Montero Moreno, A.; González González, M.; Ojeda Calvo, R.; Villanueva Romero, E.; Rubio Faure, C.; Martín García, L.; Gómez-Morón, A.; Fernández Ruiz, E. *Proyecto de conservación Cristo de la Expiración Marcos Cabrera y Juan Díaz, 1575*; Hermandad del Museo: Sevilla, Spain, 2012.
24. Rubio, C.; Pérez del Campo, L.; Montero Moreno, A.; González González, M. *Memoria Final de Intervención Cristo de la Expiración. Marcos Cabrera 1575*; Hermandad del Museo: Sevilla, Spain, 2013.
25. AENOR UNE-EN 16085. Conservation of Cultural Property. Methodology for Sampling from Materials of Cultural Property. General Rules. 2014. Available online: https://www.une.org/encuentra-tu-norma/busca-tu-norma/norma?c=N0053258 (accessed on 17 August 2020).
26. Lognoli, D.; Cecchi, G.; Mochi, I.; Pantani, L.; Raimondi, V.; Chiari, R.; Johansson, T.; Weibring, P.; Edner, H.; Svanberg, S. Fluorescence lidar imaging of the cathedral and baptistery of Parma. *Appl. Phys. B Lasers Opt.* **2003**, *76*, 457–465. [CrossRef]
27. Colao, F.; Caneve, L.; Fantoni, R.; Fiorani, L.; Palucci, A.; Fantoni, R.; Fiorani, L. Scanning hyperspectral lidar fluorosensor for fresco diagnostics in laboratory and field campaigns. In *Proceedings of the International Conference LACONA 7*; CRC Press: Boca Raton, FL, USA, 2008; pp. 149–155.
28. Colao, F.; Fantoni, R.; Fiorani, L.; Palucci, A. Application of a scanning hyperspectral lidar fluorosensor to fresco diagnostics during the CULTURE 2000 campaign in Bucovina. *Rev. Monum. Istor./Rev. Hist. Monum.* **2006**, *LXXV*, 53–61.
29. Colao, F.; Caneve, L.; Fiorani, L.; Palucci, A.; Fantoni, R.; Ortiz, M.P.; Gómez, M.A.; Vázquez, M.A. Report on Lif Measurements in Seville. Part 1: Virgen Del Buen Aire Chapel. In *Rapporti Tecnici della ENEA*; ENEA: Roma, Italy, 2012; Volume 11, pp. 1–30.
30. Colao, F.; Caneve, L.; Fiorani, L.; Palucci, A.; Fantoni, R.; Ortiz, M.P.; Gómez, M.A.; Vázquez, M.A. Report on LIF measurements in Seville—Part 2: Santa Ana Church. In *Rapporti Tecnici della ENEA*; ENEA: Roma, Italy, 2012; Volume 8, pp. 1–29.
31. Caneve, L.; Colao, F.; Fantoni, R.; Fiorani, L.; Fornarini, L. Compact scanning hyperspectral lidar fluorosensor for the discrimination of varnishes and consolidants. In *Proceedings of the International Workshop-SMW08 "In Situ Monitoring of Monumental Surfaces"*; CNR: Florence, Italy, 2008.
32. Fornarini, L.; Caneve, L.; Colao, F.; Fantoni, R.; Fiorani, L. Laser induced fluorescence analysis of acrylic resins used in conservation of cultural heritage. In Proceedings of the OSAV'2008, 2nd Int. Topical Meeting on Optical Sensing and Artificial Vision, St. Petersburg, Russia, 12–15 May 2008; pp. 57–63.
33. Access, Research and Technology for the Conservation of the European Cultural Heritage | EU-ARTECH Project | FP6 | CORDIS | European Commission. Available online: https://cordis.europa.eu/project/id/506171/es (accessed on 29 April 2020).
34. Cultural heritage Advanced Research Infrastructures: Synergy for a Multidisciplinary Approach to Conservation/Restoration | CHARISMA Project | FP7 | CORDIS | European Commission. Available online: https://cordis.europa.eu/project/id/228330 (accessed on 29 April 2020).

35. Gómez-Morón, M.A. *Estudio estratigráfico de capas pictóricas del Cristo de la Expiración*; Hermandad del Museo: Sevilla, Spain, 2012.
36. Kovala-Demertzi, D.; Papathanasis, L.; Mazzeo, R.; Demertzis, M.A.; Varella, E.A.; Prati, S. Pigment identification in a Greek icon by optical microscopy and infrared microspectroscopy. *J. Cult. Herit.* **2012**, *13*, 107–113. [CrossRef]
37. KIRBY, J.; SPRING, M.; HIGGITT, C. The Technology of Red Lake Pigment Manufacture: Study of the Dyestuff Substrate. *Natl. Gall. Tech. Bull.* **2005**, *26*, 71–87.
38. VV.AA. Artists' Pigments. In *A Handbook of Their History and Characteristics*; Feller, R.L., Ed.; Archetype Publications: London, UK, 2012; Volume 1, ISBN 978-1-904982-74-6.
39. VV.AA. Artists' Pigments. In *A Handbook of Their History and Characteristics*; Fitzhugh, E.W., Ed.; Archetype Publications: London, UK, 2012; Volume 3, ISBN 978-1-904982-75-3.
40. Acquaviva, S.; D'Anna, E.; De Giorgi, M.L.; Della Patria, A.; Pezzati, L. Optical characterization of pigments by reflectance spectroscopy in support of UV laser cleaning treatments. *Appl. Phys. A* **2008**, *92*, 223–227. [CrossRef]
41. Bruni, S.; Cariati, F.; Consolandi, L.; Galli, A.; Guglielmi, V.; Ludwig, N.; Milazzo, M. Field and Laboratory Spectroscopic Methods for the Identification of Pigments in a Northern Italian Eleventh Century Fresco Cycle. *Appl. Spectrosc.* **2002**, *56*, 827–833. [CrossRef]
42. Fotakis, C.; Anglos, D.; Couris, S. Laser Diagnostics of Painted Artworks: Laser-Induced Breakdown Spectroscopy in Pigment Identification. *Appl. Spectrosc.* **1997**, *51*, 1025–1030.
43. Welcomme, E.; Walter, P.; Bleuet, P.; Hodeau, J.L.; Dooryhee, E.; Martinetto, P.; Menu, M. Classification of lead white pigments using synchrotron radiation micro X-ray diffraction. *Appl. Phys. A Mater. Sci. Process.* **2007**, *89*, 825–832. [CrossRef]



© 2020 by the authors. Licensee MDPI, Basel, Switzerland. This article is an open access article distributed under the terms and conditions of the Creative Commons Attribution (CC BY) license (http://creativecommons.org/licenses/by/4.0/).